FISEVIER

Contents lists available at ScienceDirect

Polymer Degradation and Stability

journal homepage: www.journals.elsevier.com/polymer-degradation-and-stability





Polyphenylene sulfide for high-rate composite manufacturing: Impacts of processing parameters on chain architecture, rheology, and crystallinity

Lina N. Ghanbari ^a, Erin R. Crater ^b, Nicholas R. Enos ^a, Olivia D. McNair ^a, Robert B. Moore ^b, Jeffrey S. Wiggins ^a, *

ARTICLE INFO

Keywords:
Polyphenylene sulfide
Degradation
Rheology
Crystallization
Crystal structure
Recycling

ABSTRACT

High performance semi-crystalline thermoplastics necessitate high temperature processing to form useful structures, but the effects of repeated exposure to these extreme environments on key polymer properties are not well understood. This work investigates the influence of degradation-driven structural changes resulting from exposure to standard melt processing conditions in oxygen rich environments on the rheological properties, crystallization behavior, and crystal structure of polyphenylene sulfide (PPS). Melt processing temperatures (300°C, 320°C, and 340°C) and hold times (up to 60 min) are varied to probe the effects of thermal exposure on polymer properties. Extended melt-state exposure causes an increase in PPS melt viscosity due to the formation of complex branched/crosslinked structures where increasing temperature causes this process to occur more rapidly. Dynamic isothermal rheology of PPS displays a 70x increase in the complex viscosity at 10 rad/s after 60 minutes at 340°C. Frequency sweep rheological experiments reveal a notable deviation from linearity (terminal slope = 2) with slopes as low as 0.14 after thermal exposure. Stress recovery experiments indicate thermally processed PPS requires more time to relax stress under an applied strain. Imperfections along the polymer backbone in the form of branches/crosslinks decrease overall crystallinity and reduce lamellar thickness, with no changes to the unit cell structure. For semi-crystalline high performance thermoplastic matrix composites relying on high degrees of crystallinity to provide solvent resistance and strength, these results have serious implications for the need to tightly control melt processing steps and understand the final material state. Furthermore, viscoelastic properties of post-processed PPS polymers should be considered for recycling and reuse strategies.

1. Introduction

Semi-crystalline thermoplastic matrix composites (TPCs) are emerging high performance materials due to their chemical resistance, toughness, improved shelf life, and recyclability [1–3]. Unlike traditional thermoset matrix composites that require multifunctional monomers to cure into glassy networks, TPCs can simply be processed in the melt-state. TPCs are particularly attractive for next generation composite manufacturing as they empower economical transportation, storage, and high-rate out-of-autoclave processing. Similar to other thermoplastic manufacturing methods (i.e. injection molding and extrusion), TPCs are processed by heating beyond their melting point ($T_{\rm m}$) to transition from the crystalline state into the viscous flow state before external forces are applied to shape parts that can be demolded upon cooling and recrystallization. For composite applications, linear

high molecular weight polymers are applied to fiber reinforcements in the melt-state and are then assembled into preforms before heating (consolidation), reshaping (thermoforming), and cooling to form finished parts.

At every step of the TPC manufacturing cycle, the polymer matrix is exposed to temperatures above $T_{\rm m}$; this includes 1) unidirectional tape fabrication, 2) tape lay-up and laminate consolidation, 3) heating the consolidated preform, and 4) stamp forming [4]. Furthermore, if two finished TPC parts are to be joined via fusion bonding, additional heating is required. Once the TPC structure is ready for use, the duration which the polymer matrix sustained temperatures above $T_{\rm m}$ can be over an hour. The final thermoplastic-based structure is conceptually recyclable once decommissioned; however imprudent exposure to processing temperatures can generate undesirable material properties.

Polyphenylene sulfide (PPS) is a desirable TPC polymer matrix due to

E-mail address: Jeffrey.Wiggins@usm.edu (J.S. Wiggins).

^a School of Polymer Science and Engineering, University of Southern Mississippi, Hattiesburg, MS 39406, United States

^b Department of Chemistry and Macromolecules Innovation Institute, Virginia Tech, Blacksburg, VA, 24061, United States

 $^{^{\}ast}$ Corresponding author.

Fig. 1. Polyphenylene sulfide repeat unit.

its low cost, rapid crystallization kinetics, workable melt viscosity, high stiffness, and degree of crystallinity (~60%) afforded by its simple arylsulfide backbone (Fig. 1) [5–7]. PPS composites are traditionally melt processed at temperatures between 300°C and 340°C. For high-rate applications they are formed in an ambient, oxygen-rich atmosphere. When polymers are exposed to high energy events such as melt processing, vulnerable covalent bonds can break along the polymer backbone and form radicals through chain scission and subsequent chain transfer events, becoming facilitators for branching and crosslinking [8-10]. Recently, zero mass loss melt-state degradation mechanisms such as chain extension and branching of poly (ether ketone ketone) (PEKK) above T_m in the presence of air was determined to alter polymer crystallization and rheological behavior [11]. It is well known that similar degradation occurs in PPS but the phenomena is exacerbated by the relatively lower bond dissociation energy of the phenyl-sulfide linkage in the polymer backbone and its higher sensitivity to atmospheric oxygen, making material properties dependent on the thermal history [12-15].

The molecular alteration of PPS backbone structure due to exposure between the glass transition temperature (T_g) ($\sim\!90^\circ\text{C}$) and T_m ($\sim\!280^\circ\text{C}$) has been referred to as thermal treatment [16], annealing [17], curing [18,19], and ageing [20–22]. PPS similarly undergoes structural changes when subjected to processing temperatures above T_m . Scobbo investigated exposure conditions between 315°C and 335°C for 3 hours and 7 hours, while Joshi and Radhakrishnan studied temperatures greater than 350°C [23,24]. Both studies established that thermal exposure influenced PPS backbone architecture, but these cases focused on time scales and temperatures that do not reflect TPC melt processing conditions of PPS. In 2022, Yan and coworkers identified the thermal

degradation mechanism of PPS at melt processing temperatures in both nitrogen and oxygen rich atmospheres using X-ray photoelectron spectroscopy, Fourier-transform infrared spectroscopy, gel permeation chromatography, and dynamic rheology [25]. In air, degradation events were catalyzed by the presence of oxygen resulting in the formation of sulfoxide and sulfone groups along the PPS backbone, and aryl-ether crosslinking functional groups were observed. With increasing temperature, more extreme degradation ensued, leading to increased melt viscosity, reduced spherulite size, and an insoluble gel fraction. This seminal work provided systematic evidence of the thermal degradation mechanism of PPS at a range of melt processing temperatures but did not identify the evolution of viscoelastic behavior, crystallization, and resulting semi-crystalline morphology throughout TPC processing which are vital factors for fusion bonding and recycling, as well as chemical resistance and strength.

This paper elucidates the effects of standard melt processing conditions specific to PPS-based TPCs with an emphasis on key process and property dependent parameters: rheology and crystallinity. In this work, viscoelastic behavior, crystallization, and crystal structure of PPS were investigated after isothermal exposure to temperatures within the melt processing range (300°C, 320°C, and 340°C) for durations up to 60 minutes. Polymer structure connectivity, flow behavior, crystallization kinetics, percent crystallinity, and semi-crystalline morphology of PPS were identified through parallel plate rheology, differential scanning

Table 1Frequency and process temperature dependent complex viscosity.

Frequency (rad/s)	Temperature (°C)	η* at 0 min (Pa·s)	η* at 60 min (Pa·s)	x Increase
10	300	276.3	2725.9	9.8x
	320	183.6	4057.3	22.1x
	340	108.4	7640.7	70.7x
40	300	255.2	900.3	3.5x
	320	166.4	1209.1	7.2x
	340	89.1	2077.5	23x
80	300	239.6	567.3	2.3x
	320	160.5	717.2	4.5x
	340	88.6	1135.2	12.8x

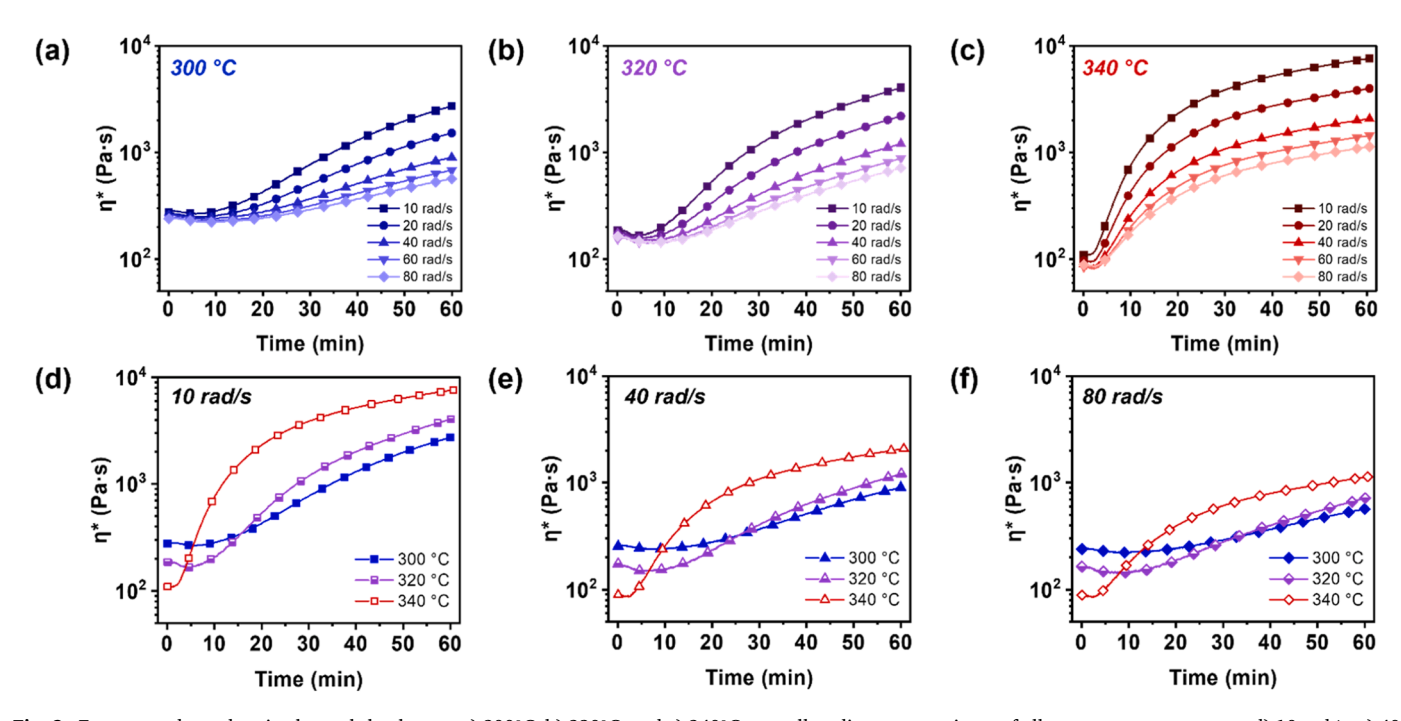


Fig. 2. Frequency dependent isothermal rheology at a) 300°C, b) 320°C, and c) 340°C, as well as direct comparisons of all process temperatures at d) 10 rad/s, e) 40 rad/s, and f) 80 rad/s.

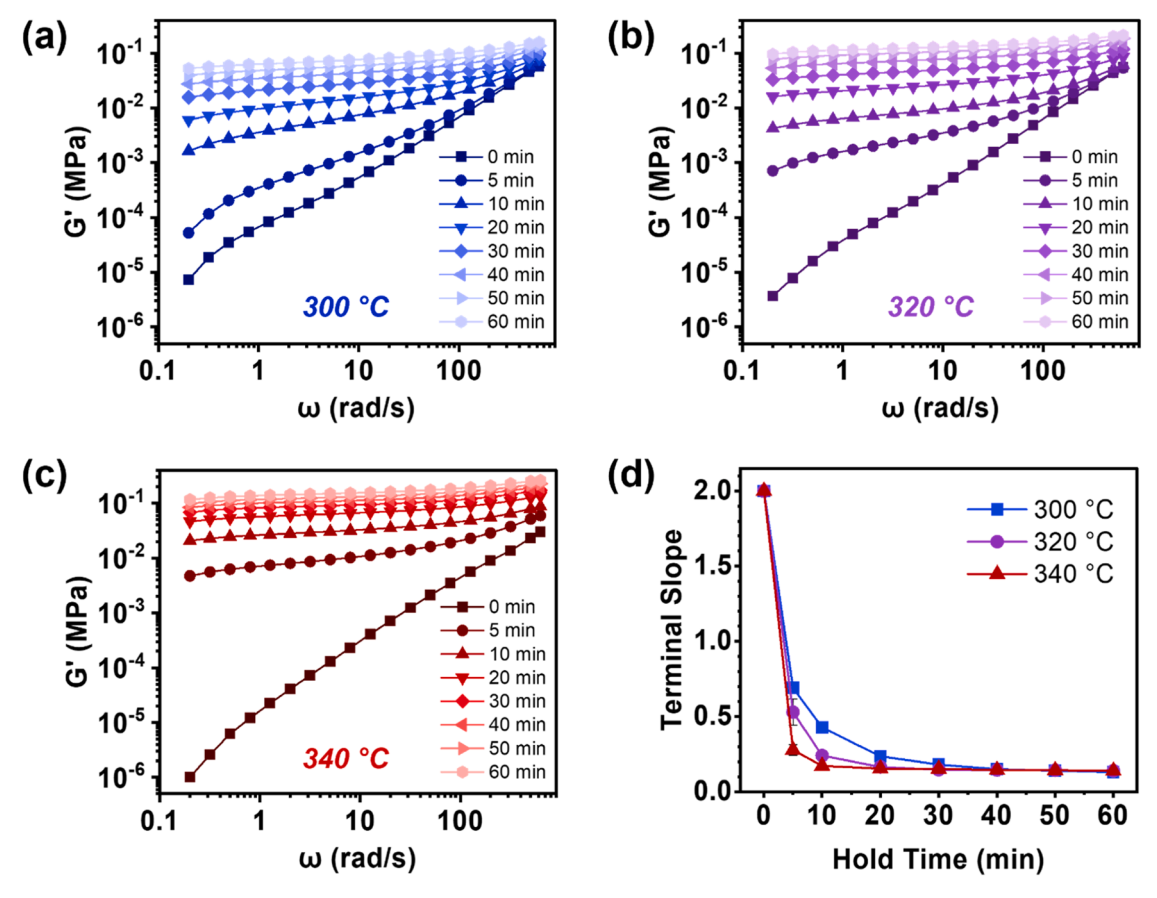


Fig. 3. Evolution of storage modulus as a function of angular frequency for PPS held at a) 300°C, b) 320°C, c) 340°C, and d) terminal slope as a function of hold time at 300°C (■), 320°C (●), and 340°C (▲). All frequency sweeps were conducted at 290°C after exposure to the process temperature for the specified amount of time.

calorimetry (DSC), and small/wide angle X-ray scattering (SAXS/WAXS).

2. Characterization

2.1. Materials

Experiments were conducted with commercially sourced PPS, Ryton® PPS QA200P (Solvay Materials). Initial thermal scans of asreceived PPS measured via DSC revealed a $T_{\rm m}$ at 282.3°C and a peak crystallization temperature (T_c) at 243.7°C, when heated/cooled under nitrogen at $10^{\circ}\text{C/min}.$ All testing of PPS in this study was conducted below the onset of mass loss thermal degradation at 494°C (Fig. S1a), and near-zero mass loss degradation of PPS was observed via isothermal TGA at 340°C (Fig. S1b).

2.2. Rheology

Melt-state viscoelastic studies were performed on a TA Instruments ARES-G2 rheometer equipped with 25 mm (isothermal and frequency sweep tests) or 8 mm (stress recovery tests) stainless steel parallel plates in the presence of air with a gap of 0.7 mm. All rheological tests were conducted within the linear viscoelastic regime (Fig. S3). Three, 1 hour isothermal multi-wave frequency measurements were conducted at 300°C, 320°C, or 340°C with frequencies ranging from 10 rad/s to 80 rad/s and corresponding strains from 0.25% to 3%. Structural evolution of the PPS melt throughout processing was analyzed by conducting frequency sweeps from 0.2 rad/s to 628 rad/s with 5% strain. Stress recovery experiments were then conducted by applying a constant strain of 10% and monitoring the induced stress. Frequency sweep and stress recovery experiments were conducted at 290°C after incremental

controlled exposure (5 to 10 minutes, up to one hour) to processing temperatures (**Fig. S2**). Measurements were taken at 290°C to directly compare results between processing temperatures and minimize thermal history acquired during the experiment.

Dynamic mechanical analysis (DMA) experiments were also performed on an ARES-G2 rheometer using 8 mm stainless steel parallel plates. PPS was loaded onto the plates and rapidly heated to melting temperatures of either 300°C, 320°C, or 340°C for 5 to 10 minutes with gap of 1 mm. Samples were cooled from the initial temperature to 40°C at 10° C/min with a frequency of 10 rad/s and 3% strain. At 247° C the strain was adjusted from 3% to 0.1% to account for material stiffening during crystallization. This cycle was repeated until the PPS samples were held at the processing temperature for a total of 60 minutes.

2.3. Differential scanning calorimetry (DSC)

Crystallization and melting events were examined using non-isothermal heating and cooling in a TA Instruments Q2500 DSC. PPS pellets were reduced to ~2-3 mg and placed in a Tzero aluminum pan/lid before heating to 340°C and holding for 3 minutes in a nitrogen environment to erase thermal history. Samples were then cooled to 70°C and heated to either 300°C, 320°C, or 340°C. Once at temperature, the cell environment was switched to air and the sample was held for 5 minutes, after which the environment was switched back to nitrogen and the sample was cooled to 50°C (**Fig. S2**). All ramp rates were set to 10° C/min. Cycles were repeated until each PPS sample was exposed to the process temperature for a total of one hour, generating 12 heating and cooling curves for each experiment. Percent crystallinity (χ) was calculated using Equation 1, where $\Delta H_{\rm C}$ is the measured enthalpy of crystallization of the sample, and $\Delta H_{\rm C}^0$ is the theoretical enthalpy for 100% crystalline PPS (79.496 J/g for PPS) [26,27].

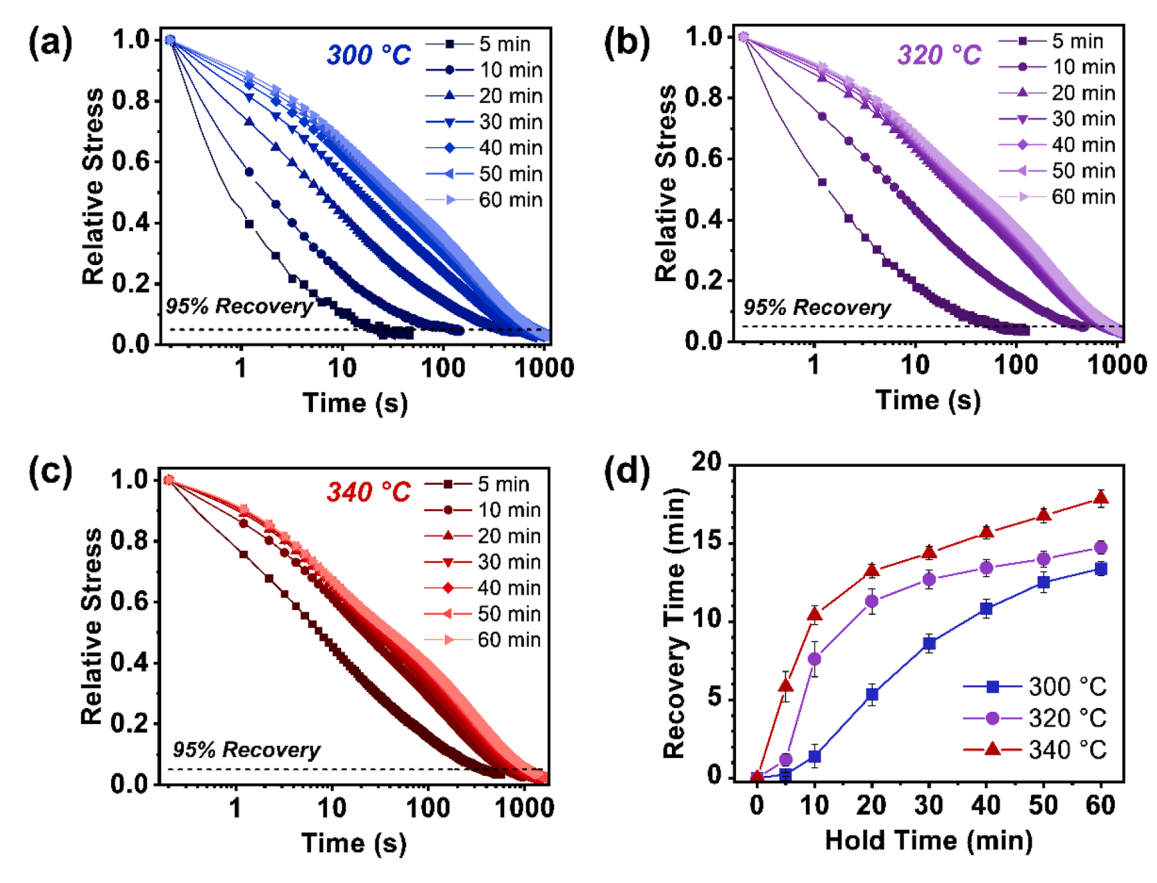


Fig. 4. Stress recovery at 290°C after processing at a) 300°C, b) 320°C, c) 340°C, and d) recovery time as a function of hold time at 300°C (■), 320°C (●), and 340°C (▲).

$$\chi = \frac{\Delta H_{\rm C}}{\Delta H_{\rm C}^0} \times 100\% \tag{1}$$

2.4. Small and wide angle X-ray scattering (SAXS/WAXS)

Samples for scattering analysis were prepared via DSC in Tzero aluminum DSC pans. Samples were prepared identically to DSC analysis, where thermal history was first erased, then the samples were subjected to the process temperature (300°C, 320°C, or 340°C) for 0 (neat PPS), 30 or 60 minutes, and finally cooled to 50°C at 10°C/min. The samples were removed from the DSC pans using a thin razor blade for scattering analysis at room temperature. Transmission small, mid, and wide-angle X-ray scattering (SAXS/MAXS/WAXS) experiments were performed on a Xenocs Xeuss 3.0 SAXS/WAXS equipped with a GeniX 3D Cu HFVLF microfocus X-ray source utilizing Cu K α radiation ($\lambda=0.154$ nm). The sample-to-detector distance was 43 mm for WAXS, 370 mm for MAXS, 900 mm for SAXS, and the q-range was calibrated using lanthanum hexaboride and silver behenate standards. Two-dimensional scattering patterns were obtained using a Dectris EIGER 4M detector with various exposure times (SAXS: 3 hours, MAXS: 2 hours, WAXS: 1 hour) (Fig. S7-9). Data reduction via azimuthal integration was performed using XSACT software provided by Xenocs, and the 1D profiles were corrected for sample thickness, background, transmission, and absolute intensity. The SAXS and MAXS profiles were merged into one dataset (hereafter referred to as "SAXS" profiles) and plotted on an absolute intensity scale versus the scattering vector, q. The WAXS profiles were plotted separately as relative intensity versus the scattering angle 20. The scattering profiles were analyzed via the 1D correlation function in SasView (Fig. S10).

3. Results

3.1. Viscoelastic behavior – frequency dependence, deviations from linearity, and stress recovery

Parallel plate rheology was implemented to monitor the real-time viscoelastic behavior and chain structure of PPS during exposure to various processing conditions. During TPC manufacturing, the shear environment is not constant, steps such as stamp forming or unidirectional tape manufacturing are inherently high shear (high frequency) processes, compared to fusion bonding which is a low shear (low frequency) process, while initial preform consolidation falls in between. Insitu multi-wave frequency experiments were used to capture the complex viscosity (η^*) of PPS for a total of 60 minutes at each processing temperature: 300°C, 320°C, or 340°C over a range of frequencies (10 rad/s to 80 rad/s) (Fig 2).

At all process temperatures, PPS demonstrated frequency-dependent viscoelastic behavior. Comparing results at 10 rad/s and 80 rad/s (representative of low and high shear TPC manufacturing processes), the 10 rad/s results displayed a 5x increase in viscosity at isothermal hold times exceeding 40 minutes compared to 80 rad/s. After one hour at 300°C, PPS showed a 9.8x increase in viscosity for 10 rad/s, compared to a 2.3x increase for 80 rad/s, while for the same time at 340°C, a 70.7x increase for 10 rad/s and a 12.8x increase for 80 rad/s were observed. At low frequencies, this viscoelastic response was linked to branching and crosslinking, which hindered the flow of chains [28]. At high frequencies, polymer shear thinning promoted chain disentanglement and decreased apparent viscosity. At longer hold times, especially at 340°C, the complex viscosity appeared to form a plateau, which was attributed to the inability of chains to form branch/crosslink sites due to diffusion limitations of reactive sites. Complex viscosities at frequencies of 10, 40, and 80 rad/s were extracted to directly compare the hold temperatures

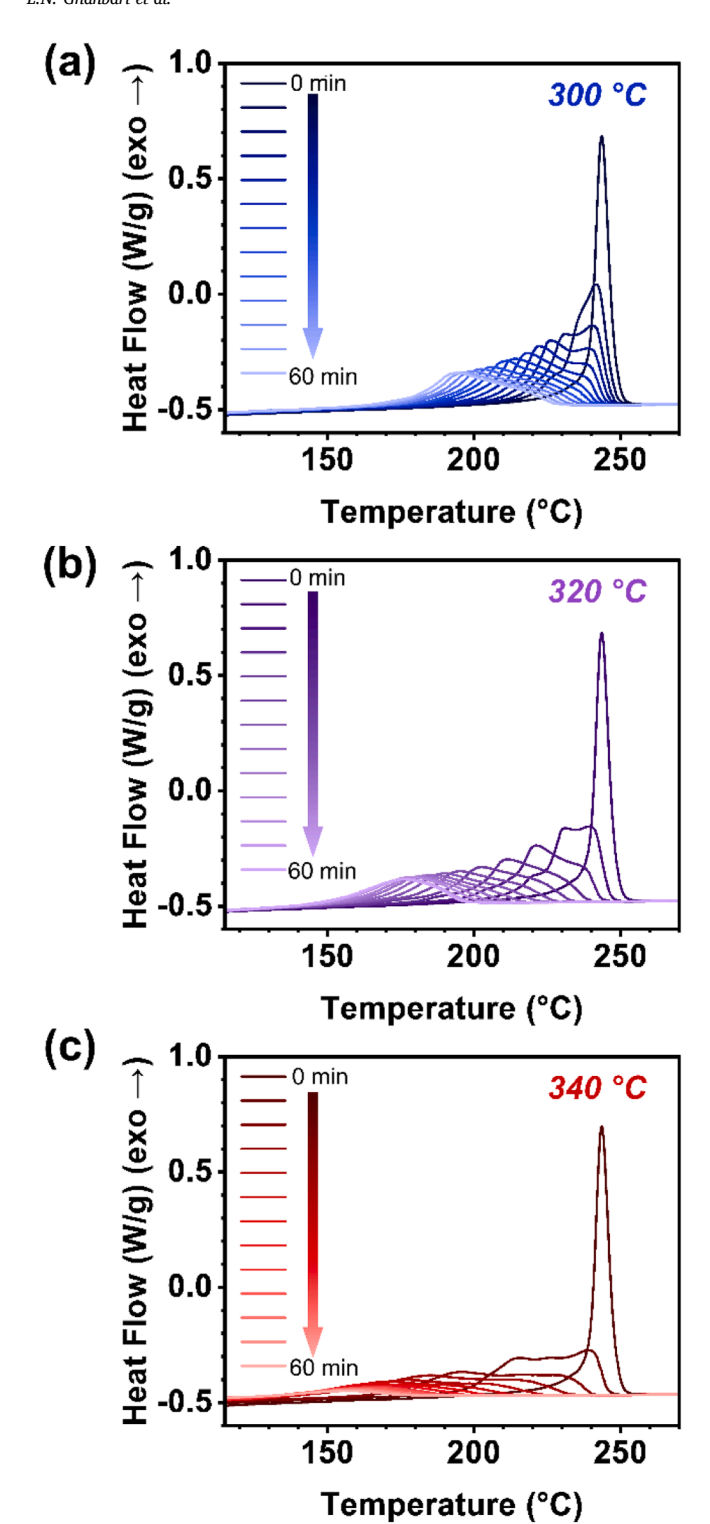


Fig. 5. DSC thermograms of PPS upon cooling from the processing temperature at 10°C/min during one hour of processing at a) 300°C, b) 320°C, and c) 340°C.

(Fig. 2d-f). At all frequencies, the complex viscosity at 0 minutes decreased with increasing hold temperature, following classical polymer melt rheology [29]. The observed decrease in complex viscosity between 0 and 15 minutes originated from initial degradation of the PPS backbone, where primary chain scission reduced the average molecular weight of the polymer melt, as discussed by Yan and Hu [25,30]. Upon further heating, complex viscosity increased sharply as radical coupling events led to branching and crosslinking. This two-step behavior was

commensurate with prior rheological studies of PPS at melt temperatures by Ma and Liu [31,32]. Viscosities at 0 minutes and 60 minutes for all frequencies and hold temperatures are listed in Table 1. At a single frequency, higher process temperatures will yield a lower polymer melt viscosity at short times; however, this behavior is inverted with prolonged exposure. The interdependencies of temperature, time, and process rate should all be considered for TPC melt processing.

Frequency sweep experiments were implemented to examine deviations from PPS linear chain structure. The slope of the storage modulus in the terminal zone (0.2 rad/s – 0.5 rad/s) can elucidate polymer backbone architecture, a method often reported for long-chain branched polymers [33–36]. When angular frequency (ω) and storage modulus (G') are plotted on a log-log scale, a perfectly linear polymer will have a terminal slope of 2, whereas a perfectly crosslinked polymer will have a terminal slope of 0 [37]. Fig. 3a-c illustrates the evolution of G' as a function of ω for hold times up to 60 minutes at 300°C, 320°C, and 340°C.

Unprocessed PPS displayed a terminal slope between 1.9 and 2, which was expected from a commercially sourced linear polymer [38]. For all hold temperatures, the terminal slope decreased with sustained thermal exposure, plateauing at 0.14 after 40 minutes which indicated evolution from a linear to branched structure (Fig. 3d). While the terminal slope values plateaued at longer hold times, the corresponding zero shear viscosity (Fig. S4) continued to increase, indicating the continued branching/crosslinking of PPS. The results displayed a strong temperature dependence of the terminal flow regime. This relationship was illustrated by the terminal slope values after five minutes at the processing temperatures: 0.69 for 300°C, 0.53 for 320°C, and 0.28 for 340°C. Comparing these terminal slopes, the rapid deviation from linear chains after processing PPS for five minutes at 320°C versus 340°C highlights non-linear temperature dependence in this regime. The rate of change in the terminal slope directly correlated to process temperature, where PPS held at higher temperatures approached a near-zero terminal slope faster than lower temperatures. These results confirmed that the isothermal rheological behavior of PPS during melt processing was due to the evolution of non-linear structures along the backbone. Polymer chains that are hindered by branching/crosslinking exhibit restricted flow will display unstable viscosity, making determination of melt processing parameters of PPS non-trivial.

The direct impacts of PPS backbone architecture on polymer chain entanglement during TPC processing was illustrated via stress recovery analysis. PPS samples were held isothermally at 300°C, 320°C, and 340°C in 5 to 10 minute intervals, then subjected to a constant 10% strain and the resulting dissipation of stress was monitored. Without normalization of the results by the initial stress in response to each strain, comparisons between samples would not be possible due to the increased stress response with prolonged holds at the processing temperature (Fig. S5). After normalization, relative stress for each sample was plotted, and the recovery time was the point at which 95% of the stress generated from the applied strain was recovered (Fig. 4a-c). For PPS with no thermal history, the stress recovery at 290°C was nearly instantaneous and within the noise of data collection (<1 second) and therefore was not included. At all processing temperatures, recovery time increased following longer hold times. Both the longer recovery times and higher initial stress upon the application of 10% strain were results of the PPS melt possessing higher elastic character due to degradation; where hindered chains resulting from branching/crosslinking possessed restricted flow, therefore requiring more time to reentangle and dissipate stress [39].

A more rapid increase in the recovery time of PPS was apparent with increasing process temperature (Fig. 4d). This rapid increase of recovery time was inversely proportional to the rapid decrease in terminal slope obtained from frequency sweep experiments, demonstrating that the formation of branched/crosslinked structures at earlier hold times due to increased hold temperature inhibited flow and mobility of the polymer melt. After 60 minutes at 300°C, 320°C, and 340°C, recovery times

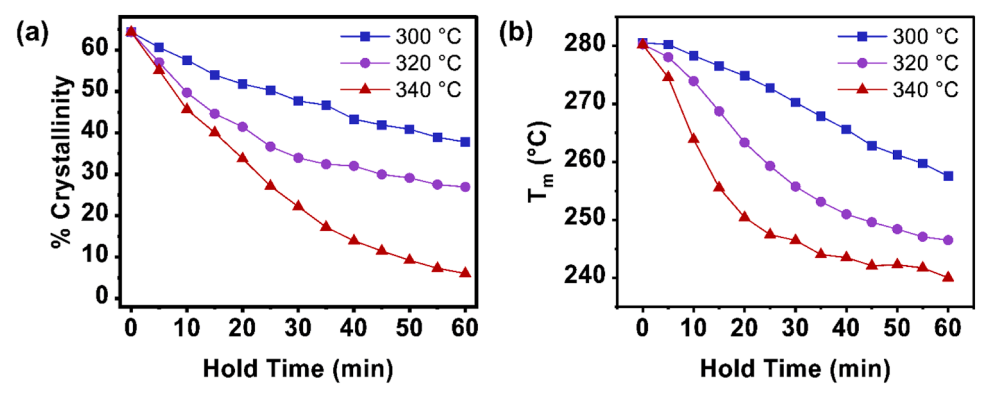


Fig. 6. a) Percent crystallinity and b) T_m as a function of hold time at $300^{\circ}C$ (\blacksquare), $320^{\circ}C$ (\bullet), and $340^{\circ}C$ (\blacktriangle).

were 13, 15, and 19 minutes, respectively. In high-rate manufacturing applications, these recovery times can be used as a model for diffusion of polymer chains in between plies or across a TPC weld line during fusion joining applications and will be investigated in a later study.

3.2. Processing dependent crystallization

Polymer crystallization from the melt-state begins with primary nucleation, which relies on the ability of chains to create local order that can stabilize and form a crystal nucleus. Adjacent chains must subsequently diffuse to the stable nucleus to form crystal lamellae, this is referred to as crystalline growth. The ability to crystallize is enhanced by polymer backbone planarity and linearity as well as flow behavior. As chains are no longer linear resulting from process-induced structural changes, inhibited crystallization and sluggish crystallization kinetics are expected consequences. Non-isothermal crystallization experiments on PPS samples held at 300°C, 320°C, and 340°C were conducted every 5 minutes over the course of 60 minutes (Fig. 5) to simulate crystallization behavior of processed PPS.

Increasing the isothermal hold time resulted in a shift of the onset and peak crystallization temperatures (Tpeak) to lower values. With increased hold temperatures, there was a greater disparity between Tpeak at 0 minutes versus 60 minutes of exposure time. The T_{peak} for neat PPS is ~243°C when cooled at 10°C/min. After one hour at 300°C, 320°C, and 340°C, this value shifted to 194°C, 175°C, and 155°C respectively. The observed monomodal crystallization peak shifted to multi-modal with prolonged temperature exposure, indicating the formation of PPS crystals over longer time scales. In prior studies, multi-modal crystallization of PPS during non-isothermal cooling has been observed as a result of the strong melt memory effect [40]. While PPS has been shown to have a strong melt memory, we hypothesize that this change in crystallization behavior is instead due to the branching/crosslinking events that occur in PPS during melt-state exposure, where defects along the polymer chain partially hinder diffusion to growing spherulites, resulting in crystal growth occurring over a larger temperature range. Crystallization behavior of melt-processed PPS was further illustrated via polarized optical microscopy found in the Supporting Information (Fig. S6). This overall shift of crystallization to lower temperatures due to sluggish crystallization kinetics is hypothesized to result in longer manufacturing cycles to reach desired crystallinity, as lower temperatures are required in order to crystallize.

Crystalline content enhances critical high performance TPC matrix properties such as solvent resistance, stiffness, and strength. In primary structure applications, a total crystallinity of at least 20% is desired to maintain these properties [41]. The overall percent crystallinity was strongly influenced by melt processing conditions (Fig. 6a).

Across all processing temperatures, the percent crystallinity decreased as the hold time increased. Neat PPS had a percent crystallinity of $\sim\!63\pm2\%$. After one hour at 300°C, 320°C and 340°C, the

percent crystallinity was lowered to 38%, 27%, and 6.0% respectively. Overall, the marked reduction in crystalline content was observed as the hold time increased. This response was intensified with higher process temperatures, where percent crystallinity decreased more rapidly and severely.

3.3. Evolution of melting behavior

Branched/crosslinked PPS chains inhibit crystallization, where imperfections along the chain backbone reduce the packing efficiency, ultimately lowering T_{peak} and percent crystallinity. The resulting melting of these crystalline domains is also influenced, leading to inconsistent melt processing parameters for TPCs. Fig. 7 depicts the subsequent DSC heating step after each sample was crystallized following a 5-minute hold at the processing temperature.

Following the trend of T_{peak} , the T_m shifted to lower temperatures with increased hold time (Fig. 6b). Pristine PPS had a T_m of 280.5 \pm 0.2°C when heated at 10°C/min, after one hour at 300°C, 320°C, and 340°C, this value shifted to 258°C, 247°C, and 240°C respectively. After PPS was held at 340°C for 20 minutes and crystallized, a cold crystallization peak at 165°C was observed upon subsequent heating. We hypothesize that after 20 minutes of exposure to 340°C, there was a fraction of PPS chains incapable of crystallization at the applied cooling rate, and would require a slower cooling rate or isothermal crystallization to fully form.

3.4. Glass transition temperature of thermally processed PPS

Multiple accounts of PPS and PPS composite thermal aging note changes in the T_g with prolonged exposure to elevated temperatures [17, 42]. The influence of exposure to processing conditions (300°C, 320°C, and 340°C, up to 60 minutes) on the Tg of PPS was investigated with both DSC and DMA. No significant shifts in T_g of PPS were observed after exposure to melt temperatures for up to 60 minutes from either method. The T_g measured from DSC ranged between $98^{\circ}C$ - $103^{\circ}C$ with no clear trend with increased hold time or temperature (Fig. 8a). However, the step change in heat capacity increased with prolonged exposure time, inverse to the decrease in percent crystallinity (Fig. S11). It is widely accepted that only the mobile-amorphous portions of semi-crystalline polymers participate in the glass transition [41]. As PPS was further branched/crosslinked due to exposure to elevated temperatures, crystallization was hindered and the total amorphous content increased. Therefore, a higher fraction of the matrix participated in the glass transition and a greater change in heat capacity was observed.

DMA experiments indicated that the T_g (from Tan (δ) peak) remained relatively unchanged with both increased time and temperature in the melt (Fig. 8b). However, after 20 minutes of exposure at 340°C, the T_g decreased from 108°C to 103°C. The G' at 60°C decreased with increasing hold time, this phenomenon occurred more rapidly with

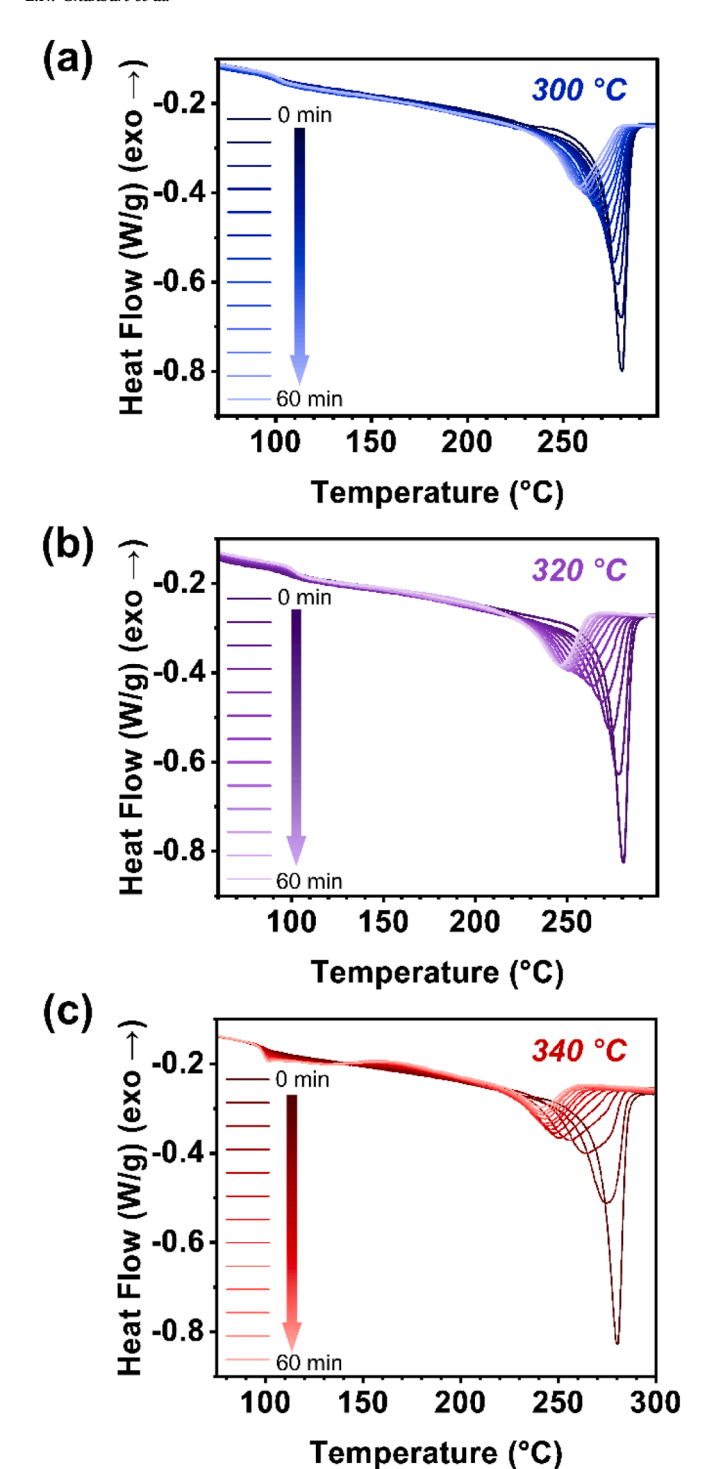


Fig. 7. DSC thermograms upon heating of PPS during one hour of processing at a) 300° C, b) 320° C, and c) 340° C.

increasing hold temperature (**Fig. S12**). The crystal domains are responsible for stiffness in semi-crystalline polymers; therefore, as PPS became more amorphous as a result of melt-state degradation, it also lost some of its rigidity, leading to a reduction in G. These results demonstrated that while oxidative degradation of PPS led to increased viscosity and amorphous content, the T_g of the mobile amorphous fraction remained largely unperturbed.

3.5. Semi-crystalline morphology resulting from varied thermal history

Given the profound effects of melt processing on the physical properties of PPS as revealed by rheology and DSC, the semicrystalline morphologies were expected to also show a strong dependence on thermal history. To investigate the effects of melt processing on the semicrystalline morphologies of PPS, SAXS and WAXS experiments were conducted on samples processed at 300 °C, 320 °C, and 340 °C in air for 0, 30, and 60 minutes and crystallized at 10 °C/min. The 1D WAXS profiles are shown in Fig. 9a-c. The diffraction pattern of neat PPS (0 min) revealed characteristic reflections of the orthorhombic unit cell reported for semicrystalline PPS (Fig. S13, Table S4) [43,44]. Moreover, the same crystalline reflections were observed in the melt processed samples, revealing that the unit cell structure was preserved upon recrystallizing samples following thermal treatment. Retention of the unit cell structure has also been observed in recrystallized samples from melt processed PEKK [11]. Therefore, it can be concluded that the long chain branches and crosslinks resulting from melt processing do not alter the unit cell structure within PPS crystallites. Despite the retention of the unit cell structure, the overall intensity of the crystalline reflections dramatically decreased with increasing processing temperature. For example, the reflection centered at $2\theta = 20.5$ corresponding to the (200) and (111) family of planes decreased in prominence when held at 300°C and 320°C for longer durations, indicating a reduction in crystallinity (Fig. 9a-b). For the samples processed at 340 °C for 30 min and 60 min, the crystalline reflections were virtually absent, likely overshadowed by the amorphous halo (Fig. 9c), further supporting that the crosslinks and branching formed at elevated processing temperatures significantly reduced the polymer's crystallizability. The trend in the percent crystallinity determined from analysis of this WAXS data was used to compare changes in percent crystallinity calculated from the DSC results. Previous studies have demonstrated that percent crystallinity determined via X-ray diffraction techniques vary compared to DSC data [45], therefore, it is important to note that the relative values for percent crystallinity based on the WAXS results herein are for comparison purposes only. Nonetheless, in both the DSC and WAXS results, percent crystallinity decreased with sustained exposure to process temperatures, this occurred at a faster rate and to a greater extent with increased temperature (Table S1, Fig. S14).

The 1D SAXS profiles are shown in Fig. 9d-f. The scattering pattern for neat PPS (0 min), revealed a strong peak centered at $q = 4.5 \text{ nm}^{-1}$, corresponding to the interlamellar long period. At longer processing times, this peak dramatically broadened into a knee-like feature due to the loss of long-range spatial order in the PPS crystallites. SAXS patterns of samples processed at 340 °C for 30 and 60 minutes (Fig. 9f) were featureless, indicating a mostly amorphous morphology. The 1D correlation function analysis was used to determine the lamellar thickness of neat PPS as 3.2 nm (Fig. S10), consistent with prior reports of melt crystallized PPS [46]. From the same analysis, PPS processed for 30 minutes at 300°C resulted in a smaller lamellar thickness of 2.6 nm. Due to the lack of crystalline order in the other melt processed samples, which displayed knee-like SAXS pattern rather than peaks, analysis from the 1D correlation function was not applicable. Consistent with the DSC analysis that showed decreasing melt temperatures as processing time increased, scattering analysis of samples held at 300°C provided additional evidence that branching and crosslinking of PPS led to thinner crystals [47]. Overall, WAXS and SAXS findings establish that melt processing reduces the overall crystallinity of PPS, and results in thinner crystallites which melt at lower temperatures.

4. Conclusions

The relationship between melt processing exposure, PPS viscoelastic behavior, crystallization, and morphology was established through rheology, DSC, and SAXS/WAXS. Isothermal rheological measurements at processing temperatures indicated initial chain scission of PPS chains

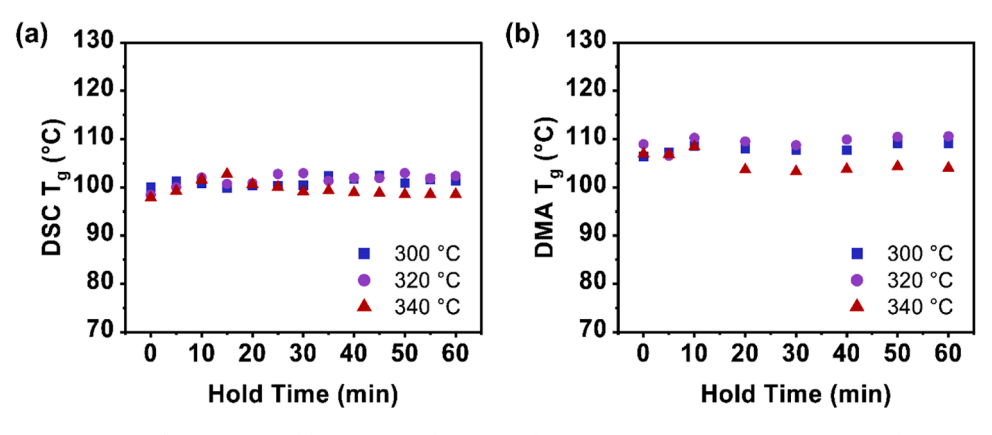


Fig. 8. Tg measured via a) DSC and b) DMA over the course of 60 minutes at 300°C (■), 320°C (●), and 340°C (▲).

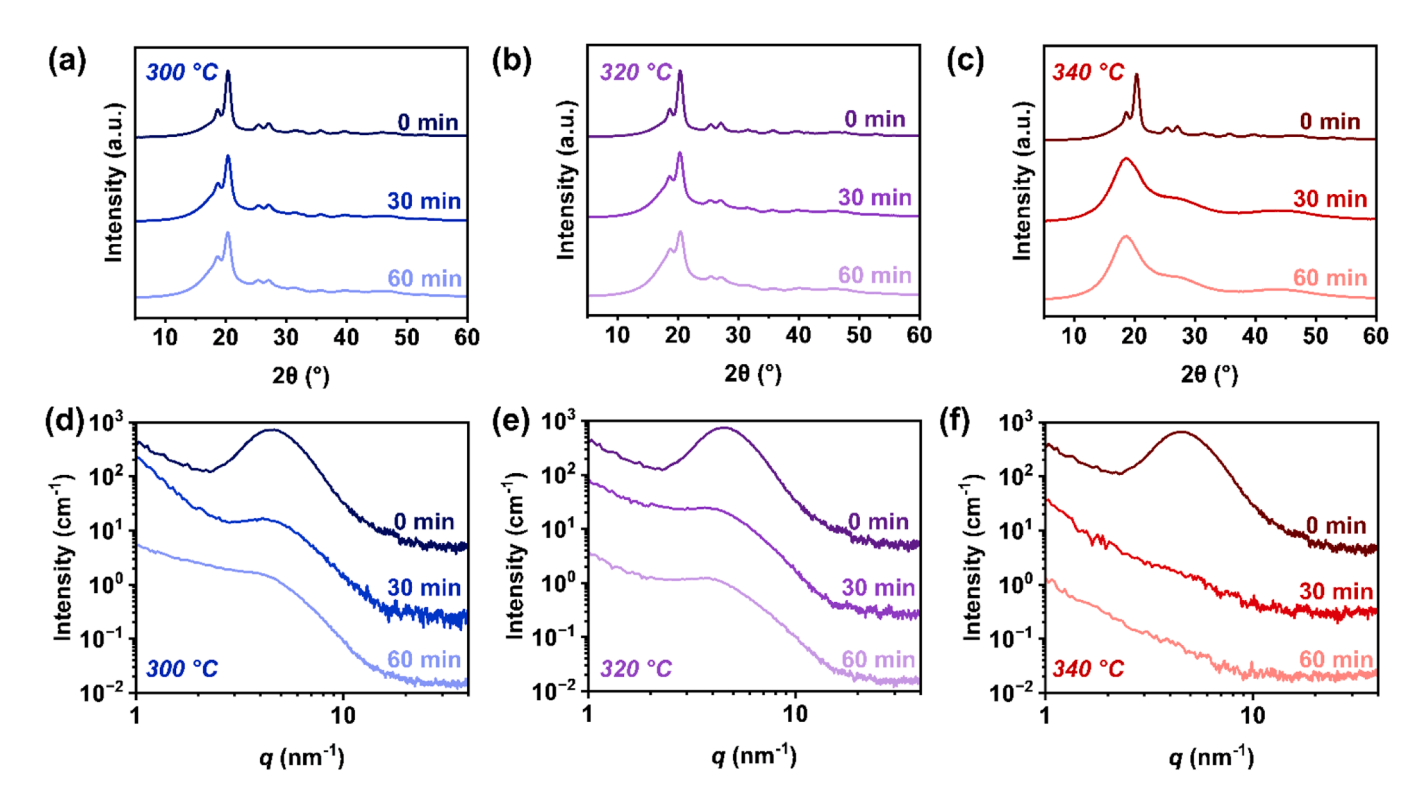


Fig. 9. 1D WAXS profiles for PPS held at a) 300° C, b) 320° C, and c) 340° C for the specified amount of time, and 1D SAXS profiles for PPS held at d) 300° C, e) 320° C, and f) 340° C for the specified amount of time. All samples were recrystallized upon cooling at 10° C/min from the specified temperature.

was rapidly followed by chain extension events, resulting in long chain branching and crosslinking. Pristine PPS was found to deviate from linearity more rapidly as the processing temperature was increased from 300°C to 340°C. Prolonged exposure to standard melt processing temperatures caused the formation of highly branched structures in PPS which led to longer stress recovery times. Percent crystallinity of PPS decreased as the hold time was increased, and the remaining crystallinity after 60 minutes of exposure was dependent on the process temperature. As the amorphous content of PPS increased, the Tg became more prominent but did not shift to lower or higher temperatures. From the DSC and SAXS results it can be stated that branching fundamentally limits crystallite thickness, while WAXS analysis shows preservation of the unit cell structure of PPS in all cases. The findings of this work allow for new considerations for designing PPS composite processing parameters - where based on rheology and DSC/X-ray scattering results, isothermal melt-state exposure in ambient environments should be limited to 30 minutes, especially at 340°C, to alleviate effects of degradation on PPS viscosity and crystallinity.

Credit Author Statement

Ms. Lina Ghanbari: Lead Researcher, Writing Original Draft, Conceptualization, Methodology, Data Curation; Ms. Erin Crater: Writing Original Draft, Data Curation, Visualization, Methodology; Mr. Nicholas Enos: Writing Original Draft, Data Curation, Visualization, Methodology; Dr. Olivia McNair: Supervision, Review and Editing; Dr. Robert Moore: Supervision; Dr. Jeffrey Wiggins: Supervision, Project Administration, Funding Acquisition

Declaration of Competing Interest

The authors have no known competing financial interests or personal relationships that influence this paper. The funding source had no influence over study design, data analysis, writing, or the decision to submit this manuscript for publication.

Data availability

Data will be made available on request.

Acknowledgements

This research was partially supported by the National Aeronautics and Space Administration (NASA) under the University Leadership Initiative program; grant number 80NSSC20M0165. Synthetic Design Synthesis of 'Thermoplastic UD Tape-based, Fastener-free assemblies' for Urban Air Mobility Vehicles; Atoms-to-Aircraft-to-Spacecraft. The authors wish to acknowledge Solvay Materials for the kind donation of PPS. Purchase of the Xenocs Xeuss 3.0 SAXS/WAXS instrument used to obtain results included in this publication was supported by the National Science Foundation under the award DMR MRI 2018258, and this research was also supported by the NSF under Grant No. 2104856. This work benefited from the use of the SasView application, originally developed under NSF award DMR-0520547. SasView contains code developed with funding from the European Union's Horizon 2020 research and innovation programme under the SINE2020 project, grant agreement No 654000.

Supplementary materials

Supplementary material associated with this article can be found, in the online version, at doi:10.1016/j.polymdegradstab.2023.110580.

References

- [1] S-S Yao, F-L Jin, KY Rhee, D Hui, S-J Park, Recent advances in carbon-fiber-reinforced thermoplastic composites: a review, Compos. Part B: Eng. 142 (2018) 241–250, https://doi.org/10.1016/j.compositesb.2017.12.007.
- [2] J Barroeta Robles, M Dubé, P Hubert, A Yousefpour, Repair of thermoplastic composites: an overview, Adv. Manuf.: Polymer Compos Science 8 (2022) 68–96, https://doi.org/10.1080/20550340.2022.2057137.
- [3] HN. Beck, Solubility characteristics of poly(etheretherketone) and poly(phenylene sulfide), J. Appl. Polym. Sci 45 (1992) 1361–1366, https://doi.org/10.1002/ app. 1992 070450806
- [4] AR. Offringa, Thermoplastic composites—rapid processing applications, Composites Part A: Appl. Sci. Manuf. 27 (1996) 329–336, https://doi.org/ 10.1016/1359-835X(95)00048-7.
- [5] G Chen, AK Mohanty, M. Misra, Progress in research and applications of Polyphenylene Sulfide blends and composites with carbons, Composites Part B: Eng. 209 (2021), 108553, https://doi.org/10.1016/j.compositesb.2020.108553
- [6] LC López, GL. Wilkes, Non-isothermal crystallization kinetics of poly(p-phenylene sulphide), Polymer 30 (1989) 882–887, https://doi.org/10.1016/0032-3861(89) 90186-9
- [7] JM Kenny, A. Maffezzoli, Crystallization kinetics of poly(phenylene sulfide) (PPS) and PPS/carbon fiber composites, Polym. Eng. Sci. 31 (1991) 607–614, https://doi.org/10.1002/pen.760310812.
- [8] AA Cuadri, JE. Martín-Alfonso, The effect of thermal and thermo-oxidative degradation conditions on rheological, chemical and thermal properties of HDPE, Polymer Degradat. Stabil. 141 (2017) 11–18, https://doi.org/10.1016/j. polymdegradstab.2017.05.005.
- [9] AD Gotsis, BLF Zeevenhoven, C. Tsenoglou, Effect of long branches on the rheology of polypropylene, J. Rheol. 48 (2004) 895–914, https://doi.org/10.1122/ 1.1764823.
- [10] Y-F Mei, B-H Guo, J. Xu, Detection of long-chain branches in polyethylene via rheological measurements, Chinese Chem. Lett. 27 (2016) 588–592, https://doi. org/10.1016/j.cclet.2016.02.023.
- [11] C Croshaw, L Hamernik, L Ghanbari, A Browning, J. Wiggins, Melt-state degradation mechanism of poly (ether ketone ketone): the role of branching on crystallization and rheological behavior, Polymer Degradat. Stabil. 200 (2022), 109968, https://doi.org/10.1016/j.polymdegradstab.2022.109968.
- [12] C Gros, J Tarrieu, V Nassiet, E. Dutarde, A study of mechanisms of poly (PhenyleneSulfide) thermal degradation in air, AMR 112 (2010) 9–17, https://doi. org/10.4028/www.scientific.net/AMR.112.9.
- [13] GFL Ehlers, KR Fisch, WR. Powell, Thermal degradation of polymers with phenylene units in the chain. II. Sulfur-containing polyarylenes, J. Polym. Sci. A-1 Polym. Chem. 7 (1969) 2955–2967, https://doi.org/10.1002/ pol.1969.150071016.
- [14] G Montaudo, C Puglisi, F. Samperi, Primary thermal degradation processes occurring in poly(phenylenesulfide) investigated by direct pyrolysis-mass spectrometry, J. Polym. Sci. A Polym. Chem. 32 (1994) 1807–1815, https://doi. org/10.1002/pola.1994.080321002.

- [15] JJ. Scobbo, Effect of solid-state curing on the viscoelastic properties of poly (phenylene sulfide), J. Appl. Polym. Sci. 47 (1993) 2169–2175, https://doi.org/ 10.1002/app.1993.070471211.
- [16] T Jimbo, S Asai, M. Sumita, Relationship between rigid amorphous fraction and structural changes of poly(phenylene sulfide) on thermal treatment, J. Macromol. Sci., Part B 36 (1997) 381–394, https://doi.org/10.1080/00222349708212391.
- [17] B Vieille, E Ernault, N Delpouve, J-DP Gonzalez, A Esposito, E Dargent, et al., On the improvement of thermo-mechanical behavior of carbon/polyphenylene sulfide laminated composites upon annealing at high temperature, Composites Part B: Eng. 216 (2021), 108858, https://doi.org/10.1016/j.compositesb.2021.108858.
- [18] G Chen, A Rodriguez-Uribe, F Wu, AK Mohanty, M. Misra, Studies on curing kinetics of polyphenylene sulfide: an insight into effects of curing temperature and time on structure and THERMO-MECHANICAL behavior, J. Appl. Polym. Sci. (2021) 51817, https://doi.org/10.1002/app.51817.
- [19] KH Lee, M Park, YC Kim, CR. Choe, Crystallization behavior of polyphenylene sulfide (PPS) and PPS/carbon fiber composites: effect of cure, Polymer Bull. 30 (1993) 469–475, https://doi.org/10.1007/BF00338482.
- [20] P Zuo, A Tcharkhtchi, M Shirinbayan, J Fitoussi, F. Bakir, Effect of thermal aging on crystallization behaviors and dynamic mechanical properties of glass fiber reinforced polyphenylene sulfide (PPS/GF) composites, J. Polym. Res. 27 (2020) 77, https://doi.org/10.1007/s10965-020-02051-2.
- [21] P Zuo, J Fitoussi, M Shirinbayan, F Bakir, A. Tcharkhtchi, Thermal aging effects on overall mechanical behavior of short glass fiber-reinforced polyphenylene sulfide composites, Polym. Eng. Sci. 59 (2019) 765–772, https://doi.org/10.1002/ peg. 25003
- [22] J Deng, Y Song, Z Xu, Y Nie, Z. Lan, Thermal aging effects on the mechanical behavior of glass-fiber-reinforced polyphenylene sulfide composites, Polymers 14 (2022) 1275, https://doi.org/10.3390/polym14071275.
- [23] JJ. Scobbo, Effect of melt-state curing on the viscoelastic properties of poly (phenylene sulfide), J. Appl. Polym. Sci. 48 (1993) 2055–2061, https://doi.org/ 10.1002/app.1993.070481118.
- [24] SG Joshi, S. Radhakrishnan, Effect of curing on the internal structure of polyphenylene sulphide coatings, Thin. Solid. Films 142 (1986) 213–226, https://doi.org/10.1016/0040-6090(86)90006-4.
- [25] P Yan, W Peng, F Yang, Y Cao, M Xiang, T Wu, et al., Investigation on thermal degradation mechanism of poly(phenylene sulfide), Polymer Degradat. Stabil. 197 (2022), 109863, https://doi.org/10.1016/j.polymdegradstab.2022.109863.
- [26] DG. Brady, The crystallinity of poly(phenylene sulfide) and its effect on polymer properties, J. Appl. Polym. Sci. 20 (1976) 2541–2551, https://doi.org/10.1002/ app.1976.070200921.
- [27] GP Desio, L. Rebenfeld, Effects of fibers on the crystallization of poly(phenylene sulfide), J. Appl. Polym. Sci. 39 (1990) 825–835, https://doi.org/10.1002/ app.1990.070390405.
- [28] T Choupin, B Fayolle, G Régnier, C Paris, J Cinquin, B. Brulé, Macromolecular modifications of poly(etherketoneketone) (PEKK) copolymer at the melting state, Polymer Degradat. Stabil. 155 (2018) 103–110, https://doi.org/10.1016/j. polymdegradstab.2018.07.005.
- [29] J Wang, RS. Porter, On the viscosity-temperature behavior of polymer melts, Rheola Acta 34 (1995) 496–503, https://doi.org/10.1007/BF00396562.
 [30] S Hu, F Yang, M Xiang, Y Cao, T Wu, Q. Fu, Competition of memory effect and
- [30] S Hu, F Yang, M Xiang, Y Cao, T Wu, Q. Fu, Competition of memory effect and thermal degradation on the crystallization behavior of polyphenylene sulfide, Polymer 262 (2022), 125427, https://doi.org/10.1016/j.polymer.2022.125427.
- [31] C-CM Ma, L-T Hsiue, W-G Wu, W-L. Liu, Rheological and morphological properties of thermal-aged poly(phenylene sulfide) resin, J. Appl. Polym. Sci. 39 (1990) 1399–1415, https://doi.org/10.1002/app.1990.070390615.
- [32] P Liu, RB Dinwiddie, JK Keum, RK Vasudevan, S Jesse, NA Nguyen, et al., Rheology, crystal structure, and nanomechanical properties in large-scale additive manufacturing of polyphenylene sulfide/carbon fiber composites, Compos. Sci. Technol. 168 (2018) 263–271, https://doi.org/10.1016/j. compscitech.2018.09.010.
- [33] SL Morelly, NJ. Alvarez, Characterizing long-chain branching in commercial HDPE samples via linear viscoelasticity and extensional rheology, Rheol. Acta 59 (2020) 797–807, https://doi.org/10.1007/s00397-020-01233-5.
- [34] P Chen, L Zhao, X Gao, Z Xu, Z Liu, D. Hu, Engineering of polybutylene succinate with long-chain branching toward high foamability and degradation, Polymer Degradat. Stabil. 194 (2021), 109745, https://doi.org/10.1016/j. polymdegradstab.2021.109745.
- [35] J Tian, W Yu, C. Zhou, The preparation and rheology characterization of long chain branching polypropylene, Polymer 47 (2006) 7962–7969, https://doi.org/ 10.1016/j.polymer.2006.09.042
- [36] H Xu, H Fang, J Bai, Y Zhang, Z. Wang, Preparation and characterization of high-melt-strength polylactide with long-chain branched structure through γ-radiation-induced chemical reactions, Ind. Eng. Chem. Res. 53 (2014) 1150–1159, https://doi.org/10.1021/ie403669a.
- [37] JD Ferry, HS. Myers, Viscoelastic properties of polymers, J. Electrochem. Soc. 108 (1961) 142C, https://doi.org/10.1149/1.2428174.
- [38] Dealy JM. Structure and rheology of molten polymers: from structure to flow behavior and back again. vol. 44. 2006.
- [39] J Guapacha, EM Vallés, LM Quinzani, MD. Failla, Long-chain branched polypropylene obtained using an epoxy resin as crosslinking agent, Polym. Bull. 74 (2017) 2297–2318, https://doi.org/10.1007/s00289-016-1839-4.
- [40] P Yan, F Yang, M Xiang, T Wu, Q. Fu, New insights into the memory effect on the crystallization behavior of poly(phenylene sulfide), Polymer 195 (2020), 122439, https://doi.org/10.1016/j.polymer.2020.122439.
- [41] S. Grove, Thermoplastic aromatic polymer composites: a study of the structure, processing and properties of carbon fibre-reinforced polyetheretherketone and

- related materials, Compos. Manuf. 4 (1993) 59, https://doi.org/10.1016/0956-7143(93)90018-4
- [42] JJ Scobbo, CR. Hwang, Annealing effects in poly(phenylene sulfide) as observed by dynamic mechanical analysis, Polym. Eng. Sci. 34 (1994) 1744–1749, https://doi. org/10.1002/pen.760342305.
- [43] BJ Tabor, EP Magré, J. Boon, The crystal structure of poly-p-phenylene sulphide, Eur. Polymer J. 7 (1971) 1127–1133, https://doi.org/10.1016/0014-3057(71) 00145 5
- [44] R Napolitano, B Pirozzi, A. Salvione, Crystal structure of Poly(p -phenylene sulfide): a refinement by X-ray measurements and molecular mechanics calculations, Macromolecules 32 (1999) 7682–7687, https://doi.org/10.1021/ ma990704x
- [45] M Doumeng, L Makhlouf, F Berthet, O Marsan, K Delbé, J Denape, et al., A comparative study of the crystallinity of polyetheretherketone by using density, DSC, XRD, and Raman spectroscopy techniques, Polymer Test. 93 (2021), 106878, https://doi.org/10.1016/j.polymertesting.2020.106878.
- https://doi.org/10.1016/j.polymertesting.2020.106878.

 [46] Y Furushima, M Nakada, Y Yoshida, K. Okada, Crystallization/melting kinetics and morphological analysis of Polyphenylene sulfide, Macromol. Chem. Phys. 219 (2018), 1700481, https://doi.org/10.1002/macp.201700481.
- [47] Q Jiang, CC Yang, JC. Li, Size-dependent melting temperature of polymers, Macromol. Theory Simul. 12 (2003) 57–60, https://doi.org/10.1002/ mats.200390003.